Quadrupole moment of the 8^+ yrast state in ^{84}Kr

R. Schwengner,[1] D. L. Balabanski,[2,*] G. Neyens,[2] N. Benouaret,[2,†] D. Borremans,[2] N. Coulier,[2] M. De Rydt,[2] G. Georgiev,[2,‡] S. Mallion,[1,2] G. Rainovski,[1,3] G. Rusev,[1] S. Teughels,[2] and K. Vyvey[2,§]

[1]*Institut für Strahlenphysik, Forschungszentrum Rossendorf, D-01314 Dresden, Germany*

[2]*Instituut voor Kern- en Stralingsfysica, Katholieke Universiteit Leuven, B-3001 Leuven, Belgium*

[3]*Faculty of Physics, St. Kliment Ohridski University of Sofia, 1164 Sofia, Bulgaria*

(Received 9 May 2006; published 8 September 2006)

The quadrupole moment of the 8^+ yrast state in ^{84}Kr was measured using the level-mixing spectroscopy technique to be $Q = 36(4)\ e\ \mathrm{fm}^2$. The result is compared with predictions of the shell model using common sets of effective charges. The comparison of experimental quadrupole moments with calculated values for 8^+ states in Kr, Sr and Zr isotopes with $N = 48$, 50 and for $9/2^+$ states in isotopes with $N = 47$, 49 suggests a modification of the effective charges used in this region.

DOI: 10.1103/PhysRevC.74.034309 PACS number(s): 21.10.Ky, 21.60.Cs, 23.20.Lv, 27.50.+e

I. INTRODUCTION

Nuclear moments are very sensitive to the structure of nuclear states and their measurement is therefore a stringent test of nuclear models. States with a structure dominated by a few nucleons outside a closed shell are good candidates for tests of predictions of the shell model. In particular, effective g factors and effective charges accounting for the influence of orbits not included in the model space may be examined.

The properties of the nuclei around the shell closure at $N = 50$ vary drastically with small changes of the nucleon numbers. Low-spin states in $N = 50$ nuclei are not collective, as indicated by measured transition strengths of $B(E2) \approx 5$ W.u. [1]. On the other hand, nuclei with two holes in the $N = 50$ shell show an onset of collectivity, which manifests itself in regular level sequences at low spin and transition strengths of $B(E2) \approx 15$ W.u. [2]. These features are well described by shell model calculations using the model space $\pi(0f_{5/2}, 1p_{3/2}, 1p_{1/2}, 0g_{9/2})\nu(1p_{1/2}, 0g_{9/2})$ [1–3]. However, a more sophisticated comparison of experimental with predicted $B(E2)$ values requires the adjustment of the effective charges for the protons and the neutrons which affects the magnitude of the calculated $B(E2)$ strengths. Because quadrupole moments involve the wave function of one state only, they are more suitable for investigating the effective charges in a given model space.

In the present work we report the first measurement of the quadrupole moment of the 8^+_1 state in the $N = 48$ nucleus ^{84}Kr using level-mixing spectroscopy (LEMS) [4,5]. The 8^+_1 state is an yrast isomer with an excitation energy of $E_x = 3236.2$ keV and a lifetime of $\tau = 2.65(6)$ μs. The measured magnetic moment of the 8^+_1 state, $\mu = -1.968(16)\mu_N$ [6], suggests a predominant $\nu(0g_{9/2}^{-2})$ configuration.

Excited states in ^{84}Kr were studied previously using the ^{82}Se$(\alpha, 2n)$ reaction [6–9] and in Coulomb excitation [10]. In a recent Coulomb-excitation experiment the quadrupole moment of the 2^+_1 state was determined [11].

II. EXPERIMENTAL TECHNIQUES AND RESULTS

The quadrupole moment of the 8^+_1 isomer in ^{84}Kr was measured at the CYCLONE facility in Louvain-la-Neuve using the LEMS technique [4,5]. In a LEMS experiment, after population and alignment of the excited nuclear states in a fusion-evaporation reaction, the recoiling nuclei are implanted into a suitable host having a non-cubic lattice, where they experience a combined electric quadrupole and magnetic dipole interaction. A split-coil superconducting magnet provides an external magnetic field of up to $B = 4.4$ T which is oriented parallel to the beam axis and thus coincides with the normal vector of the plane in which the spins are oriented after a fusion-evaporation reaction. At low strength of the magnetic field, the electric quadrupole interaction between the electric field gradient (EFG), V_{zz}, and the quadrupole moment of the isomer of interest, Q, dominate, and as a result they destroy the initial spin orientation. At a high magnetic field this interaction is negligible in comparison to the magnetic dipole interaction, and the spins perform a Larmor precession around the magnetic field $\vec{B}$. As the magnetic field is along the normal vector of the spin-orientation plane, a high field leads to an anisotropy of the intensities of isomeric transitions as induced by the spin alignment produced in a fusion-evaporation reaction. The anisotropy is measured as a function of the magnetic field, giving rise to the LEMS curve, which yields the ratio of the electric quadrupole frequency, $\nu_Q = eQV_{zz}/h$, to the magnetic interaction frequency, $\nu_\mu = \mu B/hJ$. Here, Q, μ and J are the spectroscopic quadrupole moment, the magnetic moment and the spin, respectively, of the isomer, h is the Planck constant and V_{zz} is the principal component of the electric field gradient induced by the host lattice at the site of the Kr isomer.

*Present address: Università di Camerino, I-62032 Camerino, Italy.

†Present address: Faculté de Physique, Université Alger, Alger, Algeria.

‡Present address: Centre de Spectrométrie Nucléaire et de Spectrométrie de Masse (C.S.N.S.M.), F-91405 Orsay Campus, France.

§Present address: Katholieke Universiteit Leuven, Campus Kortrijk, 8500 Kortrijk, Belgium.

The 8_1^+ isomer in ^{84}Kr was populated in the ^{82}Se(α, $2n$) reaction at an α-particle energy of 24 MeV. A three-layer target was used in the experiments. A 400 nm (432 μg/cm^2) Cd layer was evaporated onto a 80 μm (154.4 mg/cm^2) Au foil. On top of the Cd layer a 200 nm (96 μg/cm^2) layer of ^{82}Se with an enrichment of $\geqslant 95\%$ was evaporated. The ^{82}Se layer served as a production target and its thickness was chosen such that 95% of the ^{84}Kr nuclei recoiled out of it. The Cd layer served as an implantation host and the ^{84}Kr recoils were effectively stopped there, while the beam itself was stopped in the Au backing. This arrangement allowed us to utilize the maximum possible production of ^{84}Kr and to minimize the reactions in the Cd host. The beam energy is far below the Coulomb barrier of Au and as a result only transitions from Coulomb excitation of ^{197}Au were observed. In order to reduce the prompt background, a pulsed beam was used which was produced by deflecting the beam downstream from the ion source. The beam-on period was 2.5 μs, followed by a beam-off period of 9.5 μs. Data were collected in a time-gated mode as well as in a continuous mode. In the first case, events were accepted only during the beam-off period. In the latter case, singles γ-spectra were recorded in a time-integrated mode without time restrictions. Typical time-gated and nongated spectra are shown in Fig. 1. Time-gating helps in improving the peak-to-background ratios, but also reduces the intensities of the transitions because of the rather low duty cycle.

Cadmium has a hexagonal closed packed lattice. It has been chosen as a host because the EFG of Kr in Cd can be derived from the measurement of the quadrupole frequency of the ^{79}Kr, $5/2^-$ isomeric state ($T_{1/2} = 77$ ns) in Cd [12]. To deduce the electric field gradient from this frequency, the quadrupole moment of the isomer has to be known. In the table of nuclear moments by Raghavan [13], the value 45(3) e fm^2 is given, which does, however, not appear in any of the references as such. Therefore we deduced the quadrupole moment of the $5/2^-$ isomeric state in ^{79}Kr relative to that of the ^{83}Kr, $7/2^+$ state ($T_{1/2} = 147$ ns) from a measurement of the two quadrupole frequencies in a Zn crystal: $Q(^{79}\text{Kr}, 5/2^-)/Q(^{83}\text{Kr}, 7/2^+)$= 0.90(5) [14]. The quadrupole moment of the ^{83}Kr isomeric state was measured very precisely relative to that of its ground state [15] yielding a ratio of $Q(^{83}\text{Kr}, 7/2^+)/Q(^{83}\text{Kr}, 9/2^+) =$ 1.958(2). Finally, the quadrupole moment of the ^{83}Kr ground state was deduced from hyperfine-structure measurements on an atomic ^{83}Kr beam using calculated electric-field gradients [16]. In recent years, these electric field gradient calculations in combination with precise measurements of quadrupole frequencies in molecules have led to precise quadrupole moments for stable isotopes. The quadrupole moment of the ^{83}Kr ground state was deduced as $Q(^{83}\text{Kr}, 9/2^+) =$ 25.9(1) e fm^2 [17] in agreement with all earlier values, but much more precise. The combination of all these results leads to the quadrupole moments of the isomeric states in ^{83}Kr and ^{79}Kr: $Q(^{83}\text{Kr}, 7/2^+) = 50.7(3)$ e fm^2 and $Q(^{79}\text{Kr}, 5/2^-)$ $= 45.6(26)$ e fm^2, the latter being our reference for determining the quadrupole moment for the 8^+ isomeric state in ^{84}Kr.

LEMS curves from which the quadrupole frequency was deduced were obtained by measuring the anisotropies of the intensities of the isomeric γ transitions as a function of the external magnetic field. Three high-purity germanium detectors, one positioned at 0° with respect to the beam axis (i.e., along the normal axis of the spin-orientation plane and the applied magnetic field) and two positioned at 90° relative to the beam (i.e. perpendicular to the magnetic field) were used in the experiment. Because a polycrystal was used as a host, the time-integrated angular distributions of the transitions depopulating spin-aligned states remain symmetric with respect to the normal vector of the spin-alignment plane even after perturbation by the electric-quadrupole interaction, and thus the ratios of intensities measured with the detector at 0° to the beam and either of the two detectors at 90°, $N(0)/N(90_1)$ and $N(0)/N(90_2)$, lead to similar LEMS curves. Because the 882 keV transition appeared to be contaminated we used the 1078 and 1214 keV transitions only for the analysis, which led to four LEMS curves. A LEMS curve representing the average of data points obtained for the 1078 and 1214 keV transitions from the two detector combinations is shown in Fig. 2. Furthermore, both the gated and non-gated spectra were analysed resulting in a total of eight LEMS curves from which the quadrupole frequency could be derived. The fits made use of the known magnetic moment $\mu(8^+) = -1.968(16)\mu_N$ [6].

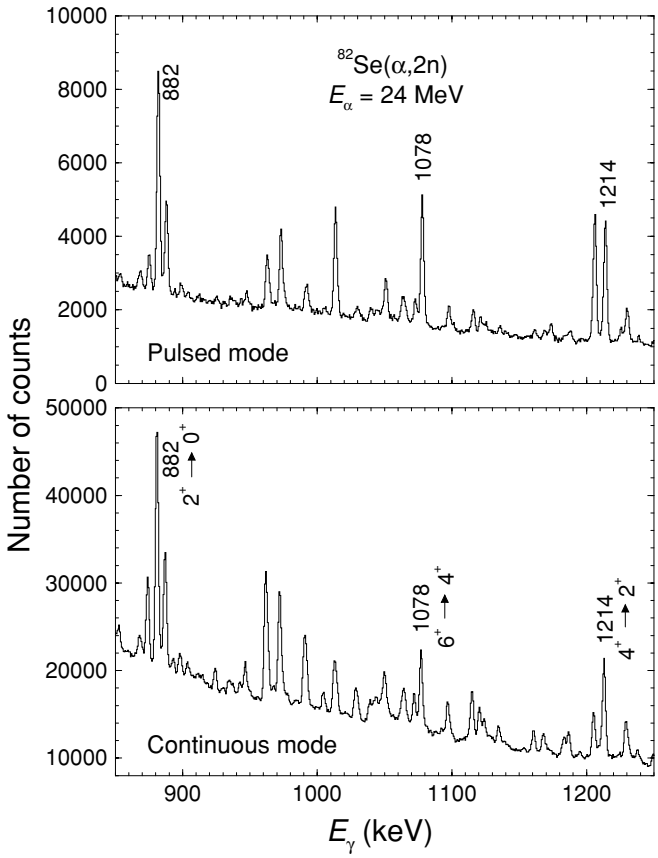

FIG. 1. Parts of γ-ray spectra measured in a time-gated (top) and continuous mode (bottom) in the ^{82}Se(α, $2n$) reaction at $E_\alpha =$ 24 MeV using a sandwiched ^{82}Se/Cd/Au target with a detector placed at 90° relative to the α-particle beam. The γ transitions used for the analysis are labeled with their energies in keV and by spins and parities of the initial and final states.

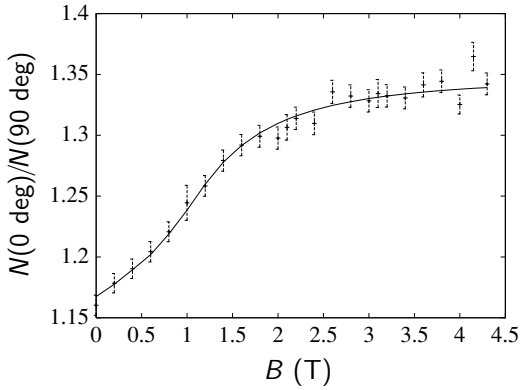

FIG. 2. LEMS curve for the 8^+ isomer in ^{84}Kr. The data points are weighted averages of the values deduced for the 1078 and 1214 keV transitions.

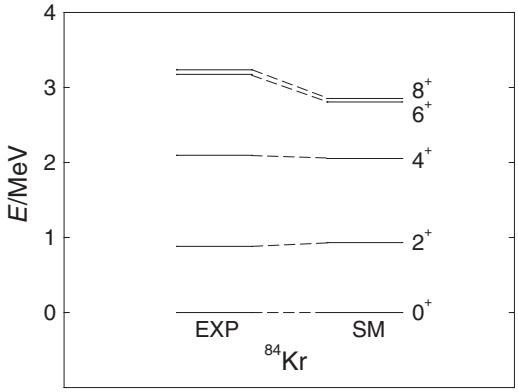

FIG. 3. Comparison of experimental and calculated level energies in ^{84}Kr.

The weighted mean of the resulting frequencies leads to a value of $\nu_Q(^{84}\text{Kr}, 8^+ \text{ in Cd}) = 35(3)$ MHz. Using the measured quadrupole frequency for the ^{79}Kr isomer in Cd, $\nu_Q(^{79}\text{Kr}, 5/2^- \text{ in Cd}) = 44.0(8)$ MHz, we obtain a quadrupole moment of $Q(^{84}\text{Kr}, 8^+) = 36(4)e$ fm^2.

III. DISCUSSION

In the following, we will compare the experimental quadrupole moments of ^{84}Kr and neighboring nuclei with predictions of the shell model. Shell-model calculations were performed using a model space including the active proton orbits $\pi(0f_{5/2}, 1p_{3/2}, 1p_{1/2}, 0g_{9/2})$ and neutron orbits $\nu(1p_{1/2}, 0g_{9/2}, 1d_{5/2})$ relative to a hypothetic ^{66}Ni core. Since an empirical set of effective interactions for this model space is not available, various empirical interactions have been combined with results of schematic nuclear interactions applying the surface delta interaction. Details of this procedure are described in Refs. [1,3]. The single-particle energies relative to the ^{66}Ni core have been derived from the single-particle energies of the proton orbits given in Ref. [18] with respect to the ^{78}Ni core and from the neutron single-hole energies of the $1p_{1/2}, 0g_{9/2}$ orbits [19]. The transformation of these single-particle energies to those relative to the ^{66}Ni core has been performed [20] on the basis of the effective residual interactions given in, e.g., Refs. [1,3]. The obtained values are $\epsilon^{\pi}_{0f_{5/2}} = -9.106$ MeV, $\epsilon^{\pi}_{1p_{3/2}} = -9.033$ MeV, $\epsilon^{\pi}_{1p_{1/2}} = -4.715$ MeV, $\epsilon^{\pi}_{0g_{9/2}} = -0.346$ MeV, $\epsilon^{\nu}_{1p_{1/2}} = -7.834$ MeV, $\epsilon^{\nu}_{0g_{9/2}} = -6.749$ MeV, $\epsilon^{\nu}_{1d_{5/2}} = -4.144$ MeV. To make the calculations feasible a truncation of the occupation number of the protons lifted to the $0g_{9/2}$ orbit to a maximum of two was applied. It turned out that neutron-core excitations of the type $\nu(0g^{-1}_{9/2}, 1d^1_{5/2})$ give only minor partitions to the wave functions of the considered states up to $N = 49$. Therefore, the calculations presented in the following include two of the neutrons in the $1p_{1/2}$ orbit and the remaining in the $0g_{9/2}$ orbit for nuclei with $N \leqslant 49$ while the core excitation $\nu(0g^{-1}_{9/2}, 1d^1_{5/2})$ was included for the $N = 50$ nuclei. With these restrictions configuration spaces with dimensions of up to 26800 were obtained. The calculations were carried out with the code RITSSCHIL [21].

Experimental and calculated level energies of the yrast states up to $J^\pi = 8^+$ in ^{84}Kr are compared in Fig. 3. There is a general agreement between experiment and calculation, although the 6^+ and 8^+ states are predicted to be about 400 keV below the experimental ones. Using effective g factors of $g_s^{\text{eff}} = 0.7 g_s^{\text{free}}$ the magnetic moment of the 8^+ state was calculated to be $\mu(8^+) = -2.12\mu_N$ which is in good agreement with the experimental value of $\mu(8^+) = -1.968(16)\mu_N$ [6].

$E2$ transition strengths and quadrupole moments have been calculated with two different sets of effective charges for protons and neutrons. The values $e_\pi = 1.35e$, $e_\nu = 0.35e$ (in the following called SM1) were adjusted to $E2$ transition strengths in nuclei around $A = 90$ in calculations using the model space $\pi(0f_{5/2}, 1p_{3/2}, 1p_{1/2}, 0g_{9/2})$ for protons and $\nu(1p_{1/2}, 0g_{9/2}, 0g_{7/2}, 1d_{5/2}, 1d_{3/2}, 2s_{1/2})$ for neutrons based on the core ^{66}Ni [22]. This set SM1 was used, e.g., in our previous shell-model studies of the isotopes ^{85}Kr$_{49}$, ^{86}Kr$_{50}$ [1], and of the nucleus ^{86}Rb$_{49}$ [3]. An alternative set of $e_\pi = 1.72e$, $e_\nu = 1.44e$ (in the following called SM2) was derived from $E2$ transitions and moments in $Z > 38$, $N = 50$ nuclei [23]. Those calculations used the model space $(1p_{1/2}, 0g_{9/2})$ for protons as well as for neutrons based on the core ^{88}Sr. This set SM2 was used, e.g., in our previous shell-model studies of nuclei with $N = 48$ [2,24], $N = 50$ [25,26], $N = 51, 52$ [27,28], and $N = 53, 54$ [29].

The results of the calculations for ^{84}Kr are compared with the experimental values in Table I. The large uncertainties of the experimental $B(E2, 2^+_1 \to 0^+_1)$ and $B(E2, 4^+_1 \to 2^+_1)$ values do not allow an evaluation of the results obtained with the different sets of effective charges. The $B(E2, 6^+_1 \to 4^+_1)$ and $B(E2, 8^+_1 \to 6^+_1)$ values are underestimated with set SM1 and overestimated with set SM2. The experimental quadrupole moment of the 2^+_1 state is reproduced by both sets within its large errors, while that of the 8^+_1 state is well reproduced with set SM1.

An interesting feature of the quadrupole moments given in Table I is the change of their sign between the 4^+_1 and the 6^+_1 states. All calculated states from 0^+_1 to 8^+_1 have the main component $\pi(0f^6_{5/2}1p^2_{3/2})\nu(1p^2_{1/2}0g^8_{9/2})$, where the spins

TABLE I. Experimental and calculated quadrupole transition strengths and moments of ^{84}Kr.

J_i^π	J_f^π	$B(E2)_{exp}/e^2fm^4$		$B(E2)_{calc}/e^2fm^4$		$Q_{exp}(J_i)/e$ fm^2		$Q_{calc}(J_i)/e$ fm^2	
		Ref. [9]	Ref. [11]	SM1	SM2	Ref. [11]	LEMS	SM1	SM2
2_1^+	0_1^+	306^{+197}_{-87}	240±30	115	389	–26(13)		–18	–33
4_1^+	2_1^+	481±87	530±70	112	394			–5.2	–11
6_1^+	4_1^+	148^{+52}_{-31}		68	254			+4.7	+9.5
8_1^+	6_1^+	48±2		25	96		36(4)	+35	+67

of the states are generated from the $0g_{9/2}$ neutron orbits only. The change of the sign of the quadrupole moment is therefore caused by the successive recoupling of the spins of two unpaired $0g_{9/2}$ neutrons from an antiparallel coupling in the 0_1^+ state to a full alignment in the 8_1^+ state. The main component of the 8_1^+ state has a partition of 30% and all partitions without proton excitations amount to 56%. The proton excitations in the remaining partitions also contribute to the quadrupole moment, which prevents a separate extraction of the effective charge for neutrons from the comparison of experimental and calculated quadrupole moments of this state.

In Table II and Fig. 4 we compare quadrupole moments calculated with the present model space for Kr, Sr and Zr isotopes with $N = 47$–50 and experimental values taken from Ref. [30]. As can be seen in Fig. 4, the trends of the calculated quadrupole moments with changing neutron numbers agree with the experimental ones. The increase of the experimental quadrupole moments of the $9/2^+$ when going from ^{83}Kr ($N = 47$) to ^{85}Kr ($N = 49$) is well reproduced by these calculations. The $9/2^+$ in ^{83}Kr is dominated by the configuration $\pi(0f_{5/2}^4 1p_{3/2}^4)_0 \nu(1p_{1/2}^2 0g_{9/2}^7)_{9/2}$, whereas the $9/2^+$ state in ^{85}Kr contains mainly the configuration $\pi(0f_{5/2}^6 1p_{3/2}^2)_0 \nu(1p_{1/2}^2 0g_{9/2}^9)_{9/2}$. A similar, but not so pronounced tendency is found for the ^{85}Sr$_{47}$,^{87}Sr$_{49}$ isotopes, while in the Zr isotopes the quadrupole moment somewhat decreases from $N = 47$ to $N = 49$. The change of sign between the quadrupole moments of the 8^+ states in ^{88}Zr$_{48}$ and ^{90}Zr$_{50}$ is described very well by the calculations. The 8^+ state in the $N = 48$ isotope is dominated by the two $0g_{9/2}$

TABLE II. Experimental and calculated quadrupole moments of $^{83-86}$Kr, $^{85-88}$Sr, and $^{87-90}$Zr.

	J^π	Q_{exp}/e fm^2 Ref. [30]	Q_{calc}/e fm^2		
			SM1	SM2	SM1N
^{83}Kr$_{47}$	$9/2_1^+$	26(3)	+10	+22	+16
^{85}Kr$_{49}$	$9/2_1^+$	44(5)	+30	+54	+40
^{85}Sr$_{47}$	$9/2_1^+$	29(3)	+12	+24	+17
^{87}Sr$_{49}$	$9/2_1^+$	34(2)	+19	+42	+30
^{87}Zr$_{47}$	$9/2_1^+$	42(5)	+12	+25	+18
^{89}Zr$_{49}$	$9/2_1^+$	28(10)	+13	+34	+24
^{84}Kr$_{48}$	8_1^+	36(4)[a]	+35	+67	+49
^{86}Kr$_{50}$	8_1^+	–	–4.6	–0.23	–0.91
^{86}Sr$_{48}$	8_1^+	–	+24	+53	+38
^{88}Sr$_{50}$	8_1^+	–	–38	–54	–42
^{88}Zr$_{48}$	8_1^+	51(3)	+19	+47	+34
^{90}Zr$_{50}$	8_1^+	–51(3)	–56	–81	–62

[a]This work.

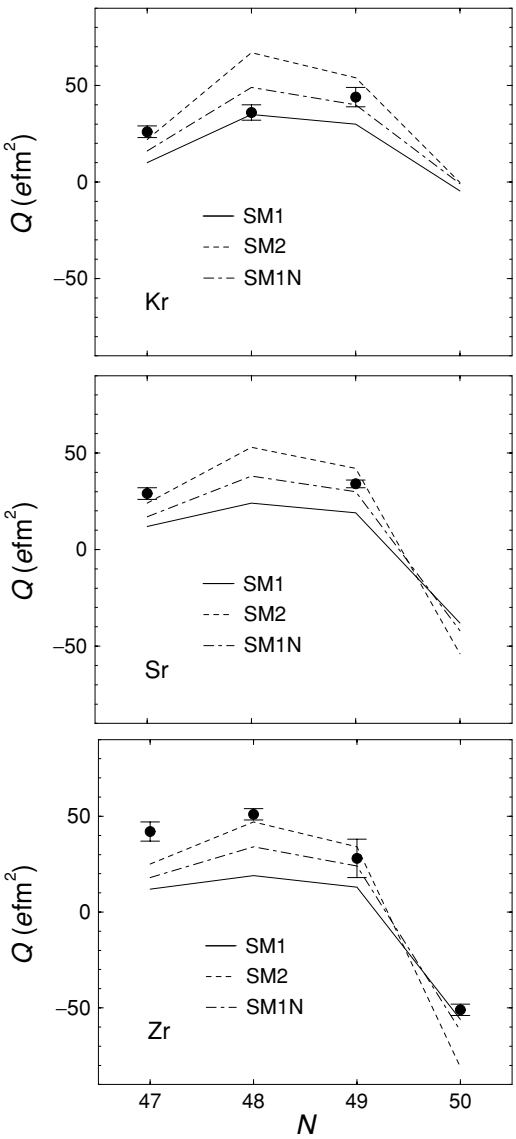

FIG. 4. Comparison of experimental and calculated quadrupole moments for $9/2^+$ and 8^+ states in the Kr, Sr and Zr isotopes with $N = 47$–50. The calculations were performed with different sets of effective charges as described in the text.

neutron holes, whereas the 8^+ state in ^{90}Zr is created by the excitation of two protons from the $1p_{1/2}$ to the $0g_{9/2}$ orbit. This is confirmed by the small negative magnetic moment $\mu = -2.26\mu_N$ calculated for the 8^+ state in ^{88}Zr and the large positive magnetic moment of $\mu = +10.1\mu_N$ calculated for the 8^+ state in ^{90}Zr which are in agreement with the experimental values $\mu(8^+,{}^{88}\text{Zr}) = -1.81(2)\mu_N$ and $\mu(8^+,{}^{90}\text{Zr}) = +10.84(6)\mu_N$ [30]. An analogous behavior is predicted for $^{86}\text{Sr}_{48}$ and $^{88}\text{Sr}_{50}$. In $^{86}\text{Kr}_{50}$, however, the 8^+ state is dominated by the configuration $\pi(0f_{5/2}^6 1p_{3/2}^2)_2\nu(1p_{1/2}^2 0g_{9/2}^9 1d_{5/2}^1)_6$ that includes a neutron-core excitation instead of the excitation of protons to the $0g_{9/2}$ orbit.

The comparison of the experimental quadrupole moments with those calculated with sets SM1 and SM2 in Table II and Fig. 4 shows that SM1 underestimates the values of the neutron-dominated isomeric states while SM2 overestimates the proton-dominated configuration in ^{90}Zr. This may indicate that the effective proton charge is too large in SM2 and the effective neutron charge is too small in SM1. In order to obtain a better overall agreement between experimental and calculated values we have introduced a new set called SM1N. This set uses the same effective charge for protons as SM1, $e_\pi = 1.35e$, but a modified effective charge for neutrons of $e_\nu = 1.0e$. The quadrupole moments calculated with SM1N are also given in Table II and Fig. 4. They show that the larger effective charge for neutrons improves the overall agreement with the experimental quadrupole moments of the neutron-dominated states, in particular for the Sr and Kr isotopes.

IV. SUMMARY

We have measured the quadrupole moment of the 8_1^+ state in ^{84}Kr for the first time by using the LEMS technique. The experimental quadrupole moment was compared with predictions of the shell model. It is shown that the quadrupole moment is very sensitive to the model space and the effective charges. Tendencies of quadrupole moments with changing neutron numbers in Kr, Sr and Zr isotopes with $N = 47$–49 are qualitatively reproduced by calculations using common sets of effective charges. The overall agreement between experimental and calculated quadrupole moments of neutron-dominated states in those nuclides is improved with a modified effective charge for neutrons. This modification of the effective charge is, however, a phenomenological way to improve the systematics applied instead of an enlargement of the configuration space which is not feasible within the present shell-model approach.

ACKNOWLEDGMENTS

This work was supported by the European Commission within the FP5 Access to Research Infrastructures programme under contract No. HPRICT199900110.

[1] G. Winter, R. Schwengner, J. Reif, H. Prade, L. Funke, R. Wirowski, N. Nicolay, A. Dewald, P. von Brentano, H. Grawe, and R. Schubart, Phys. Rev. C **48**, 1010 (1993).
[2] R. Schwengner, G. Winter, J. Reif, H. Prade, L. Käubler, R. Wirowski, N. Nicolay, S. Albers, S. Eßer, P. von Brentano, and W. Andrejtscheff, Nucl. Phys. **A584**, 159 (1995).
[3] G. Winter, R. Schwengner, J. Reif, H. Prade, J. Döring, R. Wirowski, N. Nicolay, P. von Brentano, H. Grawe, and R. Schubart, Phys. Rev. C **49**, 2427 (1994).
[4] F. Hardeman, G. Scheveneels, G. Neyens, R. Nouwen, G. Sheeren, M. VanDenBergh, and R. Coussement, Phys. Rev. C **43**, 130 (1991).
[5] G. Neyens, Rep. Prog. Phys. **66**, 633 (2003).
[6] M. Zaharcu, A. Iordachescu, E. A. Ivanov, and D. Plostinaru, Rev. Roum. Phys. **22**, 877 (1977); **27**, 33 (1982).
[7] D. G. McCauley and J. E. Draper, Phys. Rev. C **4**, 475 (1971).
[8] H. Rotter, J. Döring, L. Funke, L. Käubler, P. Kemnitz, P. Kleinwächter, L. O. Norlin, H. Prade, R. Schwengner, G. Winter, A. E. Sobov, A. P. Grinberg, I. Kh. Lemberg, A. S. Mishin, L. A. Rassadin, and I. N. Chugunov, Phys. Lett. **B163**, 323 (1985).
[9] H. Rotter, J. Döring, L. Funke, L. Käubler, H. Prade, R. Schwengner, G. Winter, A. E. Zobov, A. P. Grinberg, I. Kh. Lemberg, A. S. Mishin, L. A. Rassadin, I. N. Chugunov, A. D. Efimov, K. I. Erokhina, V. I. Isakov, L. O. Norlin, and U. Rosengard, Nucl. Phys. **A514**, 401 (1990).
[10] J. Keinonen, K. P. Lieb, H. P. Hellmeister, A. Bockisch, and H. Emling, Nucl. Phys. **A376**, 246 (1982).
[11] A. Osa, T. Czosnyka, Y. Utsuno, T. Mizusaki, Y. Toh, M. Oshima, M. Koizumi, Y. Hatsukawa, J. Katakura, T. Hayakawa, M. Matsuda, T. Shizuma, M. Sugawara, T. Morikawa, and H. Kusakari, Phys. Lett. **B546**, 48 (2002).
[12] H. Haas and H. H. Bertschat, Hyperfine Interact. **9**, 273 (1981).
[13] P. Raghavan, At. Data Nucl. Data Tables **42**, 189 (1989).
[14] H. Haas, Hahn-Meitner-Institut, Berlin, Annual Report 1977, **HMI-261** (1977), p. 50.
[15] J. H. Holloway, G. J. Schrobilgen, S. Bukshpan, W. Hilbrants, and H. Dewaard, J. Chem. Phys. **66**, 2627 (1977).
[16] W. L. Faust and L. Y. Chow Chiu, Phys. Rev. **129**, 1214 (1963).
[17] V. Kello, P. Pyykko P, and A. J. Sadlej, Chem. Phys. Lett. **346**, 155 (2001).
[18] X. Ji and B. H. Wildenthal, Phys. Rev. C **37**, 1256 (1988).
[19] R. Gross and A. Frenkel, Nucl. Phys. **A267**, 85 (1976).
[20] J. Blomqvist and L. Rydström, Phys. Scr. **31**, 31 (1985).
[21] D. Zwarts, Comput. Phys. Commun. **38**, 365 (1985).
[22] M. K. Kabadiyski, F. Cristancho, C. J. Gross, A. Jungclaus, K. P. Lieb, D. Rudolph, H. Grawe, J. Heese, K. H. Maier, J. Eberth, S. Skoda, W. T. Chou, and E. K. Warburton, Z. Phys. A **343**, 165 (1992).
[23] D. H. Gloeckner and F. J. D. Serduke, Nucl. Phys. **A220**, 477 (1974).
[24] R. Schwengner, J. Reif, H. Schnare, G. Winter, T. Servene, L. Käubler, H. Prade, M. Wilhelm, A. Fitzler, S. Kasemann, E. Radermacher, and P. von Brentano, Phys. Rev. C **57**, 2892 (1998).
[25] J. Reif, G. Winter, R. Schwengner, H. Prade, and L. Käubler, Nucl. Phys. **A587**, 449 (1995).
[26] E. A. Stefanova, R. Schwengner, J. Reif, H. Schnare, F. Dönau, M. Wilhelm, A. Fitzler, S. Kasemann, P. von Brentano, and W. Andrejtscheff, Phys. Rev. C **62**, 054314 (2000).

[27] E. A. Stefanova, R. Schwengner, G. Rainovski, K. D. Schilling, A. Wagner, F. Dönau, E. Galindo, A. Jungclaus, K. P. Lieb, O. Thelen, J. Eberth, D. R. Napoli, C. A. Ur, G. de Angelis, M. Axiotis, A. Gadea, N. Marginean, T. Martinez, Th. Kröll, and T. Kutsarova, Phys. Rev. C **63**, 064315 (2001).

[28] G. Rainovski, R. Schwengner, K. D. Schilling, A. Wagner, A. Jungclaus, E. Galindo, O. Thelen, D. R. Napoli, C. A. Ur, G. de Angelis, M. Axiotis, A. Gadea, N. Marginean, T. Martinez, and Th. Kröll, Phys. Rev. C **65**, 044327 (2002).

[29] E. A. Stefanova, M. Danchev, R. Schwengner, D. L. Balabanski, M. P. Carpenter, M. Djongolov, S. M. Fischer, D. J. Hartley, R. V. F. Janssens, W. F. Mueller, D. Nisius, W. Reviol, L. L. Riedinger, and O. Zeidan, Phys. Rev. C **65**, 034323 (2002).

[30] N. J. Stone, At. Data Nucl. Data Tables **90**, 75 (2005).